Molecular Crowding Stabilizes Both the Intrinsically Disordered Calcium-Free State and the Folded Calcium-Bound State of a Repeat in Toxin (RTX) Protein

ARTICLE *in* JOURNAL OF THE AMERICAN CHEMICAL SOCIETY · AUGUST 2013

Impact Factor: 12.11 · DOI: 10.1021/ja404790f · Source: PubMed

5 AUTHORS, INCLUDING:

Orso Subrini
Institut Pasteur
7 PUBLICATIONS **32** CITATIONS
SEE PROFILE

Daniel Ladant
CNRS & Institut Pasteur
131 PUBLICATIONS **4,768** CITATIONS
SEE PROFILE

Alexandre Chenal
Institut Pasteur
57 PUBLICATIONS **1,074** CITATIONS
SEE PROFILE

JACS
JOURNAL OF THE AMERICAN CHEMICAL SOCIETY
Article
pubs.acs.org/JACS

Molecular Crowding Stabilizes Both the Intrinsically Disordered Calcium-Free State and the Folded Calcium-Bound State of a Repeat in Toxin (RTX) Protein

Ana-Cristina Sotomayor-Pérez, Orso Subrini, Audrey Hessel, Daniel Ladant,* and Alexandre Chenal*

Unité de Biochimie des Interactions Macromoléculaires, CNRS UMR 3528, Département de Biologie Structurale et Chimie, Institut Pasteur, 28 rue du Dr Roux, 75724 Paris cedex 15, France

Supporting Information

ABSTRACT: Macromolecular crowding affects most chemical equilibria in living cells, as the presence of high concentrations of macromolecules sterically restricts the available space. Here, we characterized the influence of crowding on a prototypical RTX protein, RC_L. RTX (Repeat in ToXin) motifs are calcium-binding nonapeptide sequences that are found in many virulence factors produced by Gram-negative bacteria and secreted by dedicated type 1 secretion systems. RC_L is an attractive model to investigate the effect of molecular crowding on ligand-induced protein folding, as it shifts from intrinsically disordered conformations (apo-form) to a stable structure upon calcium binding (holo-form). It thus offers the rare opportunity to characterize the crowding effects on the same polypeptide chain under two drastically distinct folding states. We showed that the crowding agent Ficoll70 did not affect the structural content of the apo-state and holo-state of RC_L but increased the protein affinity for calcium. Moreover, Ficoll70 strongly stabilized both states of RC_L, increasing their half-melting temperature, without affecting enthalpy changes. The power law dependence of the melting temperature increase (ΔT_m) on the volume fraction (φ) followed theoretical excluded volume predictions and allowed the estimation of the Flory exponent (ν) of the thermally unfolded polypeptide chain in both states. Altogether, our data suggest that, in the apo-state as found in the crowded bacterial cytosol, RTX proteins adopt extended unfolded conformations that may facilitate protein export by the type I secretion machinery. Subsequently, crowding also enhances the calcium-dependent folding and stability of RTX proteins once secreted in the extracellular milieu.

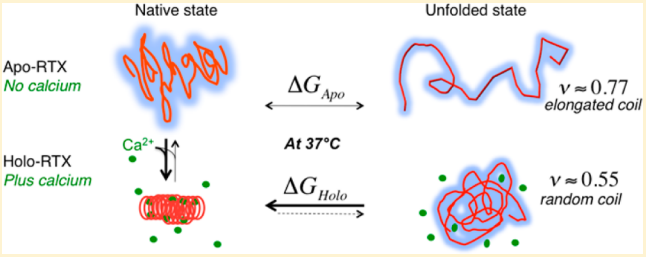

INTRODUCTION

Macromolecular crowding is a ubiquitous and fundamental characteristic of all living organisms. This concept refers to the fact that the interior of all cells is composed of a large variety of macromolecules, present at variable concentrations, that together occupy a significant fraction (20−40%) of the total intracellular volume.[1−3] The resulting steric exclusion (since a fraction of the internal space is physically inaccessible to other molecules) has consequences on both the rates and the equilibria of chemical reactions and/or associations involving macromolecules. Crowded environments affect the dynamics of proteins as they experience volume restrictions due to the surrounding macromolecules, thus restricting the allowed protein conformations. Hence, the physicochemistry of proteins (as with other biomacromolecules) in crowded environments can be markedly different from that in dilute solutions in test tubes. Macromolecular crowding may have different outcomes on protein folding and stability in vitro and in vivo.[4,5] Numerous studies, at both theoretical and experimental levels, have reported how partially folded proteins can achieve their folding to the native state in the presence of molecular crowding agents,[6−8] but only few have examined the effect of molecular crowding on intrinsically disordered proteins in vitro and in vivo.[9−15] Intrinsically disordered proteins (IDPs) are proteins characterized by structural disorder under physiological conditions, although many IDPs are able to acquire ordered conformations upon binding to ligands or to follow misfolding pathways leading to protein aggregation.[16−20]

In the present work, we carried out an extensive analysis of the effects of molecular crowding on a calcium-binding protein, RC_L that offers the rare opportunity to study the same polypeptide chain under two drastically distinct folding states: a natively unstructured state in its apo-form (R_H of 3.2 nm) and a compact folded structure in the calcium-bound form (holo-form, R_H of 2.2 nm).[21] RC_L is derived from the RTX-containing domain (Repeat in ToXin) of the adenylate cyclase toxin (CyaA) from *Bordetella pertussis*. RTX motifs are calcium-binding nonapeptide sequences (of the prototypic sequence GGXGXDX(U)X, where X represents any amino acid and U represents any large hydrophobic residue) that are found in many virulence factors produced by Gram-negative bacteria and secreted by dedicated type 1 secretion systems (T1SSs).[22] We

Received: May 13, 2013
Published: July 18, 2013

   dx.doi.org/10.1021/ja404790f | J. Am. Chem. Soc. 2013, 135, 11929−11934

previously showed that RTX polypeptides undergo a calcium-dependent disorder-to-order transition that is mainly driven by electrostatic forces.[21] In the apo-state, the negative charges of the aspartic residues of the RTX motifs repel each other and force the polypeptide chain to adopt disordered premolten globule conformations, while, in the holo-form, the bound calcium ions partly neutralize the aspartate negative charges and allow the folding of the polypeptide into a compact and stable parallel β-roll structure.[23] We proposed that the intrinsically disordered states of the RTX proteins in their apo-form may facilitate their secretion through the T1SS into the extracellular medium where, upon calcium binding, they fold into their active cytotoxic conformation.

As the structural and hydrodynamic properties of RC_L in both the calcium-free and calcium-bound states have been well characterized, this protein constitutes an attractive model to investigate the effect of molecular crowding on ligand-induced protein folding. In this study, we first explored whether molecular crowding might trigger the calcium-induced folding of this RTX protein. We showed that the crowding agent Ficoll70 did not affect the structural content of the apo- or holo-state of RC_L but increased the protein affinity for calcium. Moreover, Ficoll70 strongly stabilized both the apo- and holo-states of RC_L, increasing their half-melting temperature, T_m, by 15 and 20 °C, respectively, without affecting the enthalpy (ΔH_{vH}). These results suggest that molecular crowding reduces the conformational entropy of the protein. Finally, we discuss the experimental observation that the unfolded state of the apo-state is particularly favorable for protein secretion through the T1SS.

MATERIALS AND METHODS

Reagents and Protein Production and Purification. Experiments were performed at 25 °C in 20 mM Hepes, 100 mM NaCl, pH 7.4 (buffer A). All reagents were of the highest purity grade. Ficoll70, with an average molecular mass of 70 kDa, was purchased from Sigma-Aldrich and used without further purification.

The RC_L construct corresponds to residues 1530−1680 of CyaA (see Figure S1, Supporting Information). Plasmid construction, protein production, and purification have been previously described.[21,24]

Biophysical Techniques. Synchrotron radiation circular dichroism (SR-CD) spectra were recorded on the DISCO beamline at the synchrotron facility SOLEIL (Gif-sur-Yvette, France). Fourier transform infrared spectroscopy and fluorescence measurements were acquired, respectively, on an FP-6100 Jasco spectrometer and an FP-6200 spectrofluorimeter (Jasco) as described previously.[25,26] A further description of SR-CD, FTIR, fluorescence experiments, and fitting procedures is provided in the Supporting Information.

RESULTS

Ficoll70 Does Not Affect the Secondary Structure of RC_L. To gain insight into the effect of molecular crowding on the folding of the RTX proteins, we investigated the secondary structure of RC_L (a folding domain of CyaA made of 10 tandemly repeated, calcium-binding RTX motifs;[21,24,27] see Figure S1, Supporting Information) in the presence of increasing concentrations of Ficoll70 by SR-CD in the far-UV region. In the absence of Ficoll70, the far-UV SR-CD spectrum of RC_L in the apo-state (i.e., in the absence of calcium) was typical of disordered proteins, as shown by the strong negative $\pi-\pi^*$ band around 200 nm and a weak and broad negative $n-\pi^*$ band around 220 nm, suggesting the presence of residual secondary structure elements (Figure 1A, bold line). Upon addition of 5 mM calcium, secondary structures were formed as revealed by the concomitant intensity changes of the $\pi-\pi^*$ band (190−210 nm) and of the $n-\pi^*$ band (210−250 nm) (Figure 1B, bold line), in agreement with previous data.[24] As shown in Figure 1A, addition of Ficoll70 up to a concentration of 400 g/L did not induce any detectable change in the SR-CD spectra of apo-RC_L, indicating that Ficoll70 is not able to trigger significant secondary structure formation of the RTX motifs in the absence of calcium. Similarly, addition of Ficoll70 (100−400 g/L) did not change the secondary structure content of the calcium-bound holo-RC_L. FTIR spectroscopy further confirmed that the addition of up to 200 g/L Ficoll70 did not induce significant secondary structural changes in apo-RC_L or holo-RC_L (Figure S2 and Table S1, Supporting Information).

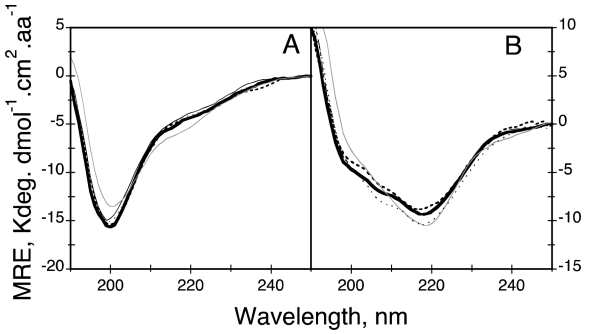

Figure 1. Effect of Ficoll70 on the secondary structure of RC_L. Far-UV SR-CD spectra of RC_L in the absence (A) or in the presence (B) of 5 mM calcium at various Ficoll70 concentrations: 0 g/L (thick line), 100 g/L (thick dashed line), 150 g/L (thin line), 200 g/L (thin dashed line), and 400 g/L (gray line). MRE = mean residual ellipticity. Experimental conditions: buffer A, 25 °C. The polypeptide concentration ranged from 200 to 350 μM.

Ficoll70 Increases the Affinity of RCL for Calcium. We next investigated the effect of molecular crowding agents on the calcium affinity (K_D) and the cooperativity of the protein folding process (n_H). The calcium-induced conformational changes of RC_L at different Ficoll70 concentrations were characterized by monitoring the ratio of the fluorescence intensities emitted at 360 and 320 nm ($FIR_{360/320}$). As shown in Figure 2A and Table S2 (Supporting Information), in the absence of Ficoll70, RC_L bound calcium with an apparent K_D of 0.53 mM. In the presence of increasing Ficoll70 concentrations, the apparent K_D of RC_L progressively decreased (see Table S2) to a value of 0.22 mM at the highest Ficoll70 concentration tested (400 g/L). These values were calculated by considering only the Ficoll70 excluded volume. Even when a Ficoll70 hydration of 0.3 g/g was assumed (resulting in an increase of the effective calcium concentrations), the calculated apparent K_D of RC_L for calcium was still significantly lower than that found in the absence of crowder molecules (e.g., apparent $K_D \approx$ 0.275 mM in the presence of 400 g/L Ficoll70, Figure 2B and Table S2). A Hill number (n_H) for calcium binding to RC_L of about 4 was found at all Ficoll70 concentrations (Figure 2B, inset), indicating that the molecular crowding agent did not affect the cooperativity of the folding process.

The increase in calcium affinity of RC_L in the presence of macromolecular crowding is consistent with the steric reduction of accessible volume and the reduction of conformational entropy. As calcium binding to RC_L is accompanied by a strong compaction of the polypeptide chain from natively disordered conformations into a folded and stable structure,[24]

dx.doi.org/10.1021/ja404790f | J. Am. Chem. Soc. 2013, 135, 11929−11934

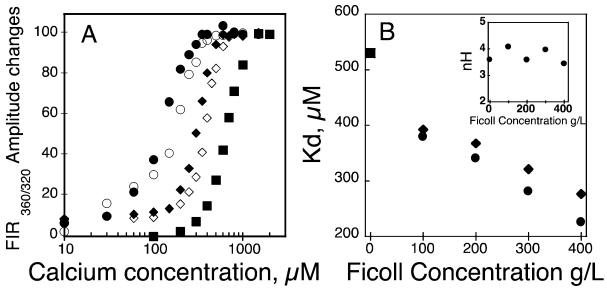

Figure 2. Effect of Ficoll70 on the calcium dissociation constant (K_D) of RC_L. (A) Ratio of fluorescence intensities at 360 and 320 nm ($FIR_{360/320}$) of RC_L as a function of the calcium concentration at different Ficoll70 concentrations: ■, 0 g/L (buffer); ◇, 100 g/L; ◆, 200 g/L; ○, 300 g/L; ●, 400 g/L. (B) K_D of RC_L as a function of the Ficoll70 concentration, considering the excluded volume of dry Ficoll70 (●) or the excluded volume of Ficoll70 with a hydration layer of 0.3 g/g (◆). Inset: Hill number (n_H) as a function of the Ficoll70 concentration. Experimental conditions: buffer A, 25 °C. The polypeptide concentration was 2.5 μM. The standard deviation is below 0.02 mM.

the excluded volume effect would favor the folded calcium-bound protein at the expense of the unfolded apo-form.

Ficoll70 Strongly Increases the Thermal Stability of RC_L. To gain insight into the stability changes of RC_L induced by Ficoll70, we investigated the thermally induced denaturation of both the apo- and holo-states by using SR-CD and tryptophan intrinsic fluorescence (Figure 3).

The thermally induced unfolding of the secondary structure of holo-RC_L was characterized by an increase of the negative $\pi-\pi^*$ band and a concomitant decrease of the $n-\pi^*$ band (Figure S3, Supporting Information). At high temperatures (>90 °C), the far-UV SR-CD spectrum of the unfolded holo-state was similar to that of the native apo-state at 25 °C (Figure 1A), exhibiting characteristics typical of a mostly disordered polypeptide with only minor residual secondary structure elements. In the presence of Ficoll70, the SR-CD spectrum of the thermally induced unfolded RC_L was similar to that recorded in the absence of Ficoll70 (compare Figure 3A and Figure S3), but the thermally induced unfolding of RC_L was shifted toward higher temperatures (Figure 3A), as shown by ellipticity changes at both 218 nm (Figure 3B) and 201 nm (Figure S4, Supporting Information). The stabilization of holo-RC_L by Ficoll70 was further assessed by tryptophan intrinsic fluorescence (Figure 3C and Figure S5, Supporting Information). At each tested concentration of Ficoll70, similar denaturation profiles of holo-RC_L were observed by both SR-CD and tryptophan intrinsic fluorescence. A two-state model was fitted to all thermal denaturation profiles (see the Supporting Information and Figure S6, Supporting Information), allowing determination of the temperature of half-melting (T_m), the van't Hoff enthalpy (ΔH_{vH}), and the heat capacity (ΔC_p). As shown in Figure 3D, the ΔH_{vH} values were similar at the different Ficoll70 concentrations tested. However, the T_m values strongly increased with the concentration of molecular crowding agents: indeed, a large increase in T_m of more than 20 °C was observed from 0 to 400 g/L Ficoll70 (Figure 3D and Table S3, Supporting Information).

Similarly, we examined the thermally induced melting of the natively disordered apo-form of RC_L. Unfolding of apo-RC_L could not be followed by SR-CD due to a lack of significant dichroic signals of this disordered polypeptide but could be

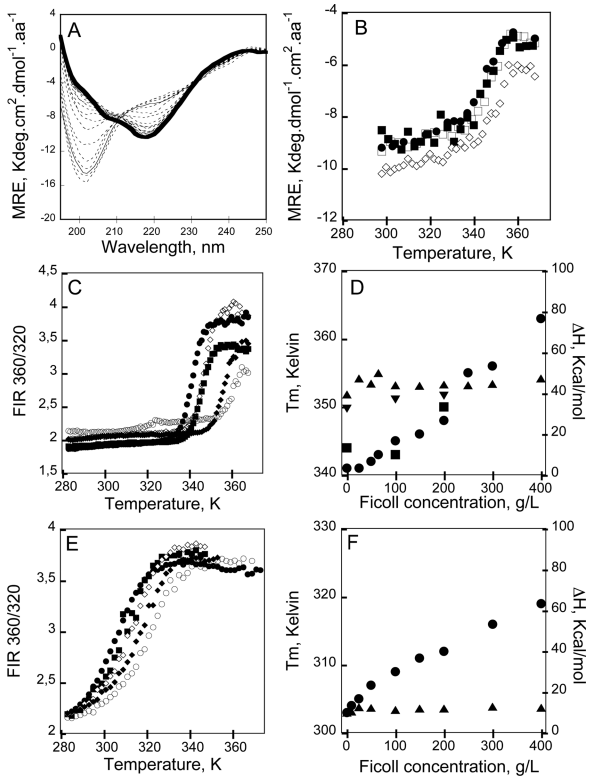

Figure 3. Effect of Ficoll70 on the thermal stability of RC_L. (A) Far-UV SR-CD spectra of holo-RC_L as a function of temperature in the presence of 200 g/L of Ficoll70. Holo-RC_L at 25 °C is bold and at 95 °C is shown as a continuous line. (B) SR-CD changes of holo-RC_L upon thermal unfolding followed at 218 nm in the presence of 0 g/L (●), 100 g/L (■), 150 g/L (□), and 200 g/L (◇) of Ficoll70. MRE = mean residual ellipticity. Experimental conditions: buffer A + 5 mM calcium. The polypeptide concentration was 200 μM. Thermal denaturation of holo-RC_L (C) and apo-RC_L (E) followed by $FIR_{360/320}$ in buffer containing 0 g/L (●), 100 g/L (■), 200 g/L (◇), 300 g/L (◆), and 400 g/L (○) of Ficoll70. Temperatures of half-melting (T_m, ●) and van't Hoff free enthalpies (ΔH_{vH}, ▲) of holo-RC_L (D) and apo-RC_L (F) as a function of Ficoll70 concentration. Experimental conditions: buffer A plus or minus 2 mM calcium. The RC_L concentration was 10 μM. Panel D shows T_m (■) and ΔH_{vH} (▼) values of Holo-RC_L extracted from SR-CD thermal denaturation data. Note that in panels D and F the ΔH_{vH} scales are identical, whereas the T_m scales have similar amplitude but different ranges. The standard deviation of T_m values is ± 1K; SD on Δ is less than 5 kcal/mol.

monitored by changes of the intrinsic fluorescence (Figure 3E). As expected for an intrinsically disordered protein, apo-RC_L exhibited a low melting temperature (T_m) of about 32 °C (see Table S3, Supporting Information, and Figure 3F) in the absence of crowding agents. In the presence of increasing Ficoll70 concentrations (from 100 to 400 g/L), a significant stabilization of the apo-form was observed. As shown in Figure 3F, the T_m markedly increased, to 46 °C, in the presence of 400 g/L Ficoll70, corresponding to a T_m increment of 16 °C from 0 to 400 g/L Ficoll70 (see Table S3). The ΔH_{vH} values, however, remained similar regardless of the Ficoll70 concentrations used (Figure 3F).

From the T_m, ΔH_{vH}, and ΔC_p values, the ΔG values of both the apo- and holo-states of RC_L were estimated for each Ficoll70 concentration at 37 °C (see the Supporting Information). Figure 4 shows that ΔG increased linearly with the Ficoll70 concentration and that Ficoll70 stabilizes both the

dx.doi.org/10.1021/ja404790f | J. Am. Chem. Soc. 2013, 135, 11929−11934

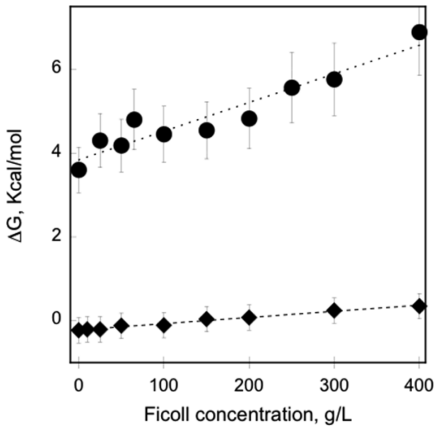

Figure 4. Ficoll70 effect on the free energy of RC_L. The ΔG values of the apo-state (◆) and of the holo-state (●) are reported at 37 °C. Data are computed from the thermodynamic values presented in Figure 3 and listed in Table S3 (Supporting Information).

apo- and holo-states of RC_L. Noteworthy, the increment of ΔG stabilization as a function of the Ficoll70 concentration (i.e., the slopes of the lines in Figure 4, amounting to 1.5 and 7 kcal/mol/M_F for apo-RC_L and holo-RC_L, respectively) clearly indicates that Ficoll70 stabilized the holo-state more than the apo-state. Overall, Figures 3 and 4 show that Ficoll70 mostly enhanced the stability of holo-RC_L through an increase of the T_m without significantly affecting the enthalpy changes. This suggests that Ficoll70 stabilizes RC_L through a reduction of the conformational entropy of RC_L rather than inducing structure formation. Altogether the thermal-denaturation data of both apo- and holo-RC_L are in agreement with the hypothesis that molecular crowding favors the more compact conformations of macromolecules.

■ DISCUSSION

In the present work we describe the effects of molecular crowding on ligand-induced folding and stability changes of an intrinsically disordered protein. According to the excluded volume theory, one of the major effects of crowding agents on macromolecules is a destabilization of the unfolded state.[28,29] Most of these models have been well studied in silico, and additional experimental validations are clearly needed.

Here, we carried out an extensive characterization of the effects of molecular crowding on a calcium-binding protein, RC_L, an RTX-containing protein, derived from the bacterial CyaA toxin. RC_L is a 155-residue polypeptide (corresponding to the isolated block V of the CyaA toxin[30]) that is intrinsically disordered in the absence of calcium and folds, upon calcium binding, into a compact and stable state.[24] The RC_L protein therefore constitutes an excellent model to investigate the effect of molecular crowding agents on the ligand-induced transition from disordered to ordered states of intrinsically disordered proteins.

We showed by SR-CD and FTIR that the addition of up to 400 g/L Ficoll70 did not induce significant conformational changes of RC_L, either in its apo-state or in its holo-state. We then demonstrated that molecular crowding increased the affinity of RC_L for calcium ions (K_D). However, it did not affect the cooperativity (n_H) of the folding process, suggesting that the calcium-induced folding is similar in the absence or presence of Ficoll70. We propose that the molecular confinement, induced by high concentrations of crowding agents, reduces the conformational entropy of the intrinsically disordered state of apo-RC_L, facilitating calcium binding to the protein by decreasing the effective free energy barrier to fold into the holo-state. In the case of RC_L, this effect might be particularly strong as calcium binding triggers a transition between two states that display markedly distinct structural, thermodynamic, and hydrodynamic properties (i.e., an intrinsically disordered state and a folded state).[24] Our data are in agreement with the suggestion that, in confining environments, the compact holo-state (R_H = 2.2 nm) should be energetically favored as compared to the disordered apo-state (R_H = 3.2 nm).[21]

We further investigated how molecular crowding affects the stability (ΔH_{vH} and T_m) of both the apo- and holo-states of RC_L upon temperature-induced denaturation. SR-CD and fluorescence data indicated that Ficoll70 does not change the ΔH_{vH} values, suggesting that the enthalpy changes and the structural content of both the apo- and holo-states are not affected by molecular crowding. Conversely, it is noteworthy that the T_m values increased for both the apo- and holo-states of RC_L as a function of the Ficoll70 concentration. As mentioned above, one of the effects of the excluded volume is to physically reduce the conformational entropy, i.e., the space available for protein conformational fluctuations. These steric constraints due to molecular confinement lead to the destabilization of the unfolded state of the protein, which consequently favors the folded state and shifts the T_m values toward higher temperatures. Moreover, it has been shown that molecular crowding excludes solvent around proteins and affects protein hydration, thus driving proteins to adopt more compact conformations.[31,32] These effects result in an entropically favorable protein stabilization, as exemplified here by the large increase of the ΔT_m of RC_L with Ficoll70. In agreement, the Ficoll70-induced ΔG changes (Figure 4) further showed that molecular crowding stabilizes the holo-state more than the apo-state, probably because the changes of molecular volume induced by temperature are larger for the holo-state than for the apo-state of RC_L.

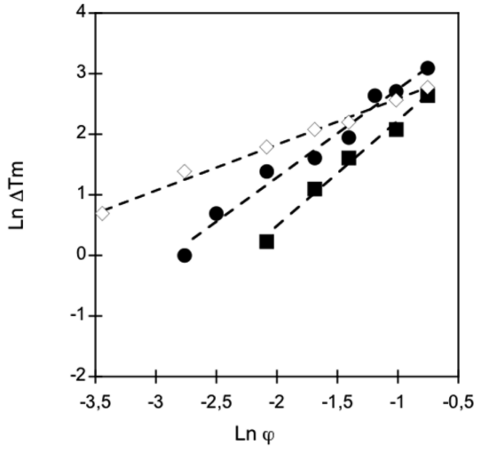

Figure 5. Ficoll70 effect on the melting temperature (ΔT_m) as a function of the Ficoll70 excluded volume (φ) using data coming from apo-RC_L (◇) and holo-RC_L thermal denaturation followed by tryptophan intrinsic fluorescence (●) and by SR-CD in the far-UV region (■). The Ficoll70 excluded volume is computed with a hydration of 0.3 g/g. See the Supporting Information for details on the φ_C calculations.

dx.doi.org/10.1021/ja404790f | J. Am. Chem. Soc. 2013, 135, 11929−11934

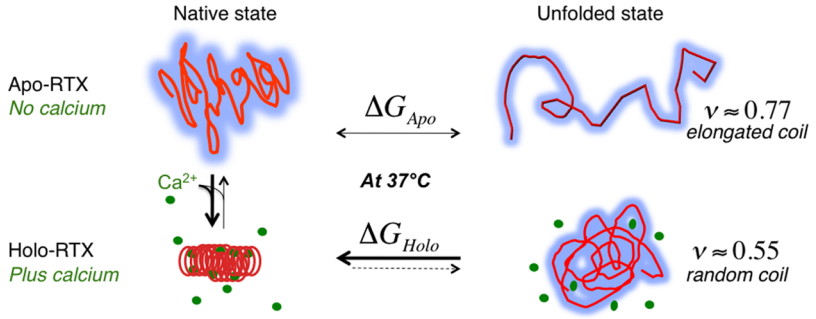

Figure 6. Conformational changes, hydrodynamics, and thermodynamics of RC_L at 37 °C. In the absence of calcium, RC_L adopts an intrinsically disordered state, while the addition of calcium induces its folding and stabilization. Molecular crowding increases the affinity of RC_L for calcium. At 37 °C, the apo state is in equilibrium between its native state and its unfolded state, while in the presence of calcium, the native holo state is highly favored in comparison to the unfolded holo state. Molecular crowding further increases the stability of the holo state. Molecular crowding studies also indicate that the unfolded holo state adopts a random coil conformation, while the unfolded apo state adopts an elongated conformation, which might be favorable to protein secretion through the type 1 secretion system (see Discussion). The protein is represented in red, calcium ions are shown in green, and protein hydration is represented in blue.

Cheung and Tirulamai proposed that the effect of molecular crowding agents on the thermal stability of proteins could be theoretically evaluated according to the size of the confinement space ($\Delta T_m = \chi^* \varphi^{\alpha/3}$), where χ is a constant (see the Supporting Information) and α a factor related to the Flory exponents ν of the unfolded states.[33] A recent in vitro study on ubiquitin supports the power-law dependence of ΔT_m on φ.[34] As shown in Figures 5 and S7 (Supporting Information), plots of ln ΔT_m as a function of ln φ follow straight lines for both apo- and holo-RC_L, the slopes of each, $\alpha/3$, being related to the Flory exponents ν according to $\nu = 1/\alpha + 1/3$ (see the Supporting Information). The calculated Flory exponent scales the gyration radius, R_G, to the length, N, of the macromolecules ($R_G = R_0 N^{\nu}$), with R_0 being a scaling factor. The ν values range from 0.3 to 0.5−0.6 for folded and unfolded proteins, respectively, and reach higher values for extended macromolecules in good solvent.[33,36] The Flory exponents ν for the thermally induced unfolded state of RC_L in the presence of calcium are 0.53 and 0.56 from SR-CD and fluorescence data, respectively (Table S4 (Supporting Information) and Figure 6). These values are in good agreement with the Flory exponent of unfolded proteins behaving in a space of three dimensions (d = 3 and $\nu \approx 0.6$) and are characteristic of random coils in good solvent conditions[37] (see the Materials and Methods and Table S4 in the Supporting Information). It is noteworthy that the Flory value for the unfolded state of RC_L in the absence of calcium is 0.77 (Table S4 (Supporting Information) and Figure 6). This suggests that the thermally induced unfolded conformations of the intrinsically disordered apo-state of RC_L are expanded, behaving like elongated polymers in a good solvent.[37] The difference between the Flory exponent values of apo-RC_L ($\nu \approx 0.77$) and holo-RC_L ($\nu \approx 0.55$) suggests that calcium is able to induce a partial collapse of the extended conformations of the heat-denatured polypeptides. Calcium may screen the electrostatic repulsion between the negatively charged aspartic acid residues of RC_L in its apo-state,[21] thus allowing a partial collapse of the polypeptide chain (Figure 6). Interestingly, other intrinsically unfolded proteins, which are highly charged at neutral pH like apo-RC_L (pI = 4.4), also appeared expanded as compared to what was found for the chemically denatured states of folded proteins.[38]

Our present results provide several novel insights into the secretion process of RTX-containing proteins. Most RTX proteins are virulence factors produced by more than 250 Gram-negative bacterial species.[22] They are all predicted to be secreted by a type I secretion machinery (T1SS) and to require calcium to exert their cytotoxicity. We previously suggested that, within the host bacteria, due to low intracellular calcium concentrations (less than micromolar), the RTX motifs are mainly unfolded, thus favoring the polypeptide secretion through the dedicated type I secretion machinery.[26] As several studies have reported that partially folded proteins can achieve their folding to the native state in the presence of molecular crowding agents,[39,40,6−8] we aimed to determine whether the crowded intracellular environment might be able to favor structural folding of an RTX-containing protein. Clearly, our present data show that the apo-state of RC_L remains intrinsically disordered and does not acquire any secondary structure in the presence of the crowding agent Ficoll70 (even at the highest concentration of 400 g/L). Molecular crowding inside bacteria is expected to range from 200 to 300 g/L biomolecules,[41] below the 400 g/L Ficoll70 tested here. Our data suggest that the RTX motifs of the T1SS protein substrates remain intrinsically disordered inside the bacteria prior to secretion, despite the highly crowded environment of the bacterial cytosol. Similar observations have been reported for other IDPs.[42]

We previously showed that, in the absence of crowding agents and at rather low concentrations, the shape of the natively disordered apo-state of RTX proteins, including RC_L, is globular.[24] However, the Flory exponent of the thermally unfolded RC_L (ν = 0.77) in the absence of calcium indicates that RTX motifs have the potential to adopt elongated conformations, similarly to stretched polymers confined in capillaries or inside slits.[36] Indeed, macromolecules diffusing in a space of two dimensions (d = 2) are characterized in a good solvent condition by a Flory exponent of 0.75[37] (see the Supporting Information), a value close to 0.77 for the thermally unfolded apo-RC_L. It is tempting to speculate that such extended conformations might contribute to an efficient uptake and passage of the polypeptide substrates through the narrow channel of the type 1 secretion machinery.

Interestingly, our thermodynamic data show that the energetic cost to fully unfold and extend apo-RC_L is rather low, between −0.3 and +0.4 kcal/mol (from 0 to 400 g/L Ficoll70; see Figure 4 and Table S3, Supporting Information) at physiological temperatures (37 °C). Hence, in the crowded bacterial cytosol, in the absence of calcium, the disordered apo-

dx.doi.org/10.1021/ja404790f | J. Am. Chem. Soc. 2013, 135, 11929−11934

state of RTX motifs may adopt elongated conformations (ν = 0.77) most favorable for secretion at essentially no energetic cost.

Finally, we showed that the affinity of RC_L for calcium in a crowded environment is favored and that its stability increases with increasing crowding agent concentration. These results strongly suggest that, during the secretion process, once the RTX polypeptide substrate exits the secretion machinery to reach the calcium-enriched extracellular medium, the holo-state is highly favored at the expense of the disordered apo-state. This transition may provide the energy for a molecular ratchet mechanism of secretion due to the difference of stability between the disordered state inside the bacteria (in a low $[Ca^{2+}]$ environment) and the stable and folded holo-state in the extracellular environment (see ΔG changes in Figure 4). Taken together, we may hypothesize that molecular crowding favors the disordered state of the RTX proteins within the bacteria and facilitates their secretion and finally their calcium-induced folding to their cytotoxic active form in the extracellular environment.

■ ASSOCIATED CONTENT

Supporting Information

Additional information on the materials and methods used in this study, additional data, Figures S1−S7, and Tables S1−S4. This material is available free of charge via the Internet at http://pubs.acs.org.

■ AUTHOR INFORMATION

Corresponding Author

alexandre.chenal@pasteur.fr; daniel.ladant@pasteur.fr

Notes

The authors declare no competing financial interest.

■ ACKNOWLEDGMENTS

We acknowledge SOLEIL for the provision of synchrotron radiation facilities (Proposal IDs 20110586 and 20120444), and we thank Frank Wien for assistance in using the DISCO beamline. We thank Scot Ouellette and Agnes Ullmann for critical reading of the manuscript. We thank all members of our laboratory for their constant interest and encouragement. The project was supported by the Institut Pasteur (Projet Transversal de Recherche, PTR#374 and DGAS), the Centre National de la Recherche Scientifique (CNRS UMR 3528, Biologie Structurale et Agents Infectieux), and the Agence Nationale de la Recherche, Programme Jeunes Chercheurs (Grant ANR-09-JCJC-0012).

■ REFERENCES

(1) Minton, A. P. *Mol. Cell. Biochem.* **1983**, *55*, 119.
(2) Ellis, R. J. *Trends Biochem. Sci.* **2001**, *26*, 597.
(3) Zhou, H. X.; Rivas, G.; Minton, A. P. *Annu. Rev. Biophys.* **2008**, *37*, 375.
(4) Dhar, A.; Samiotakis, A.; Ebbinghaus, S.; Nienhaus, L.; Homouz, D.; Gruebele, M.; Cheung, M. S. *Proc. Natl. Acad. Sci. U.S.A.* **2010**, *107*, 17586.
(5) Dhar, A.; Girdhar, K.; Singh, D.; Gelman, H.; Ebbinghaus, S.; Gruebele, M. *Biophys. J.* **2011**, *101*, 421.
(6) Zhang, D. L.; Wu, L. J.; Chen, J.; Liang, Y. *Acta Biochim. Biophys. Sin.* **2012**, *44*, 703.
(7) Perham, M.; Stagg, L.; Wittung-Stafshede, P. *FEBS Lett.* **2007**, *581*, 5065.
(8) Wang, Y.; He, H.; Li, S. *Biochem. Biokhim.* **2010**, *75*, 648.
(9) Wang, Y.; Benton, L. A.; Singh, V.; Pielak, G. J. *J. Phys. Chem. Lett.* **2012**, *3*, 2703.
(10) Cino, E. A.; Karttunen, M.; Choy, W. Y. *PLoS One* **2012**, *7*, e49876.
(11) Johansen, D.; Jeffries, C. M.; Hammouda, B.; Trewhella, J.; Goldenberg, D. P. *Biophys. J.* **2011**, *100*, 1120.
(12) Roque, A.; Ponte, I.; Suau, P. *Biophys. J.* **2007**, *93*, 2170.
(13) McNulty, B. C.; Young, G. B.; Pielak, G. J. *J. Mol. Biol.* **2006**, *355*, 893.
(14) Qu, Y.; Bolen, D. W. *Biophys. Chem.* **2002**, *101−102*, 155.
(15) Flaugh, S. L.; Lumb, K. J. *Biomacromolecules* **2001**, *2*, 538.
(16) Dunker, A. K.; Obradovic, Z. *Nat. Biotechnol.* **2001**, *19*, 805.
(17) Uversky, V. N. *Protein Sci.* **2002**, *11*, 739.
(18) Dyson, H. J.; Wright, P. E. *Nat. Rev. Mol. Cell. Biol.* **2005**, *6*, 197.
(19) Bourhis, J. M.; Canard, B.; Longhi, S. *Curr. Protein Pept. Sci.* **2007**, *8*, 135.
(20) Munishkina, L. A.; Fink, A. L.; Uversky, V. N. *Curr. Alzheimer Res.* **2009**, *6*, 252.
(21) Sotomayor-Perez, A. C.; Ladant, D.; Chenal, A. *J. Biol. Chem.* **2011**, *286*, 16997.
(22) Linhartova, I.; Bumba, L.; Masin, J.; Basler, M.; Osicka, R.; Kamanova, J.; Prochazkova, K.; Adkins, I.; Hejnova-Holubova, J.; Sadilkova, L.; Morova, J.; Sebo, P. *FEMS Microbiol. Rev.* **2010**, *34*, 1076.
(23) Baumann, U.; Wu, S.; Flaherty, K. M.; McKay, D. B. *EMBO J.* **1993**, *12*, 3357.
(24) Sotomayor Perez, A. C.; Karst, J. C.; Davi, M.; Guijarro, J. I.; Ladant, D.; Chenal, A. *J. Mol. Biol.* **2010**, *397*, 534.
(25) Chenal, A.; Karst, J. C.; Sotomayor Perez, A. C.; Wozniak, A. K.; Baron, B.; England, P.; Ladant, D. *Biophys. J.* **2010**, *99*, 3744.
(26) Chenal, A.; Guijarro, J. I.; Raynal, B.; Delepierre, M.; Ladant, D. *J. Biol. Chem.* **2009**, *284*, 1781.
(27) Szilvay, G. R.; Blenner, M. A.; Shur, O.; Cropek, D. M.; Banta, S. *Biochemistry* **2009**, *48*, 11273.
(28) de Gennes, P. G. *Scaling Concepts in Polymer Physics*; Cornell University Press: Ithaca, NY, 1979.
(29) Minton, A. P. *Biophys. J.* **2005**, *88*, 971.
(30) Bauche, C.; Chenal, A.; Knapp, O.; Bodenreider, C.; Benz, R.; Chaffotte, A.; Ladant, D. *J. Biol. Chem.* **2006**, *281*, 16914.
(31) Hong, J.; Gierasch, L. M. *J. Am. Chem. Soc.* **2010**, *132*, 10445.
(32) Harada, R.; Sugita, Y.; Feig, M. *J. Am. Chem. Soc.* **2012**, *134*, 4842.
(33) Cheung, M. S.; Klimov, D.; Thirumalai, D. *Proc. Natl. Acad. Sci. U.S.A.* **2005**, *102*, 4753.
(34) Waegele, M. M.; Gai, F. *J. Chem. Phys.* **2011**, *134*, 095104.
(35) Receveur-Bréchot, V.; Durand, D. *Curr. Protein Pept. Sci.* **2012**, *13*, 55.
(36) Sakaue, T.; Raphaël, E. *Macromolecules* **2006**, *39*, 2621.
(37) Flory, P. J. *Principles of Polymer Chemistry*; Cornell University Press: Ithaca, NY; 1953.
(38) Kohn, J. E.; Millett, I. S.; Jacob, J.; Zagrovic, B.; Dillon, T. M.; Cingel, N.; Dothager, R. S.; Seifert, S.; Thiyagarajan, P.; Sosnick, T. R.; Hasan, M. Z.; Pande, V. S.; Ruczinski, I.; Doniach, S.; Plaxco, K. W. *Proc. Natl. Acad. Sci. U.S.A.* **2004**, *101*, 12491.
(39) Homouz, D.; Perham, M.; Samiotakis, A.; Cheung, M. S.; Wittung-Stafshede, P. *Proc. Natl. Acad. Sci. U.S.A.* **2008**, *105*, 11754.
(40) Stagg, L.; Zhang, S. Q.; Cheung, M. S.; Wittung-Stafshede, P. *Proc. Natl. Acad. Sci. U.S.A.* **2007**, *104*, 18976.
(41) Record, M. T., Jr.; Courtenay, E. S.; Cayley, D. S.; Guttman, H. J. *Trends Biochem. Sci.* **1998**, *23*, 143.
(42) Szasz, C. S.; Alexa, A.; Toth, K.; Rakacs, M.; Langowski, J.; Tompa, P. *Biochemistry* **2011**, *50*, 5834.

Supporting Information to

Molecular crowding stabilizes both the intrinsically disordered calcium-free state and the folded calcium-bound state of an RTX protein

Ana-Cristina Sotomayor-Pérez, Orso Subrini, Audrey Hessel, Daniel Ladant & Alexandre Chenal

Material and Methods

Reagents

Experiments were done at 25 °C in 20 mM Hepes, 100 mM NaCl, pH 7.4 (Buffer A). All reagents were of the highest purity grade. Among several molecular crowding agents tested, we have selected Ficoll70, which even at the highest concentration tested of 400 g/L did not induce any detectable aggregation of RC_L, in the absence or in the presence of calcium.

Ficoll70, with an average molecular mass of 70 kDa, was purchased from Sigma-Aldrich (Ref F2878) and used without further purification. A stock solution at 400 g/L was prepared in buffer A. Density and viscosity of Ficoll70 at different concentrations were measured by a densimeter (Thermo Fisher) and a falling-ball viscosimeter (Gilmont), respectively.

Polypeptides production and purification

RC_L construction corresponds to residues 1530-1680 in native numbering of CyaA. Plasmid construction, protein production and purification have been described previously [1,2]. Briefly, RC_L was overproduced in *E. coli* BLR strains (Novagen, Merck KG, Darmstadt, Germany) and successively purified by chromatography on a nickel HiTrap chelating column (elution in 500 mM imidazole, 20 mM Hepes, 200 mM NaCl, pH 7.4), size exclusion chromatography on Sephacryl S200 (20 mM Hepes, pH 7.4, 100 mM NaCl) and finally by ion exchange chromatography on Q sepharose (elution with 20 mM Hepes, 500 mM NaCl pH 7.4) at room temperature. Ethylenediaminetetraacetic acid (EDTA) at a final concentration of 2 mM was added to samples before desalting on prepacked G25SF against 20 mM Hepes, 100 mM NaCl pH 7.4 (for storage at –20 °C).

Protein purity was higher than 95% as judged by SDS-PAGE. The integrity and identity of the samples was confirmed by N-terminal sequencing. Absolute molecular mass was measured by surface enhanced laser desorption/ionization time-of-flight mass spectrometry (SELDI-TOF-MS model PCS 4000, Ciphergen). SELDI experiments provided a molar mass of 17124 g. mol^{-1} and protein concentration was determined by UV spectrophotometry using molar extinction coefficient (at 280 nm) of 18 000 $M^{-1}cm^{-1}$.

SR-CD *Circular dichroism spectroscopy*

In preliminary experiments with conventional CD spectrometer (data not shown), we observed that Ficoll70 itself presented a strong negative band in the far-UV region from 190 to 210 nm. Its intensity was proportional to the Ficoll70 concentration, precluding accurate CD spectra analysis of RTX

proteins. These observations prompted us to use synchrotron radiation circular dichroism (SR-CD, DISCO beamline at the synchrotron facility SOLEIL, Gif-sur-Yvette, France). The SR-CD experiments were carried out at 25°C, integration time of 1200 msec and a bandwidth of 1 nm with a 1 nm resolution-step. Each far-UV spectrum represents the average of at least 3 scans. Optical cell with a 26 µm path-length and CaF_2 windows (Hellma) were used for recording CD signals in far-UV region (from 180 to 260 nm). Buffer A in the absence of in the presence of increasing concentrations of Ficoll70 was used as blank and its spectrum was subtracted to protein spectra. The CD units used were the mean residue ellipticity (MRE), expressed in kilodegrees square centimeter per decimole and per aminoacids ((Kdeg*cm^2)/(dmol*aa)).

The thermal-induced denaturation of the apo-state and holo-state in the far-UV region were followed from 25 to 95 °C using a water-cooled Peltier temperature controller. The temperature increased by steps of 2, 3 or 5°C. The data were processed as described previously [3].

Fourier transform infrared spectroscopy

FTIR was acquired on a FP-6100 Jasco spectrometer, equipped with a ceramic source, a Ge/KBr beam splitter and a DLATGS (Deuterated, L-alanine doped triglycine sulphate) detector. A Peltier unit regulated the temperature of the cell compartment, which was constantly purged with dried air.

The protein samples and the Ficoll70 solutions were twice lyophilized. Protein samples were solubilized in buffer A (with or without 5 mM calcium) prepared in D_2O and then mixed with a 400 g/L stock solution of Ficoll70 in D_2O. Protein concentrations ranged from 1 to 5 mg/mL.

FT-IR experiments were performed as described previously [3]. Briefly, each spectrum corresponds to the accumulation of 512 scans, recorded from 1000 to 8000 cm^{-1} at a resolution of 4 cm^{-1}. The buffer spectrum (with or without 200 g/L of Ficoll70) was subtracted from the sample spectrum prior subtraction of a scaled spectrum of CO_2 and water vapor.

The major bands of the protein FTIR spectra were then identified by standard deconvolution and second derivative procedures. The maximum wavenumber values were used to deconvolute absorption bands. A deconvoluted spectrum consists of the sum of bands, each band made of fractions of a Gaussian and of a Lorentzian curve. The residuals were below 0.3 % of the initial absorbance signal. The area under each absorption band was used to quantify the secondary structure content taking into account the molar absorption of each band and according to the following assignments [4-7]: intermolecular β-sheets (E_M= 1000 /M/cm) from 1612 to 1627 cm^{-1}, intramolecular β-sheets (E_M= 700 /M/cm) from 1625 to 1640 cm^{-1}, disordered regions (E_M= 330 /M/cm) from 1640 to 1650 cm^{-1}, α-helices (E_M= 540 /M/cm) from 1650 to 1660 cm^{-1}, turns (E_M= 300 /M/cm) between 1660 and 1680 cm^{-1}, and finally, antiparallel β-sheet (E_M= 300 /M/cm) from 1680 to 1697 cm^{-1}. All acquisitions and data processing were done using Spectra Analysis (Jasco). The deconvoluted absorption bands were plotted using Kaleidagraph (Synergy Software, Reading, PA).

Fluorescence spectroscopy

Measurements were performed using a FP-6200 spectrofluorimeter (Jasco, Japan) equipped with a Peltier-thermostated cell holder, using 2 mL samples in 1 cm path-length quartz cells (111-QS from Hellma). A bandwidth of 5 nm was used for the excitation and emission beams. RC_L concentration was 2.5 µM for calcium titration experiments and 10 µM for thermal denaturation followed by tryptophan intrinsic fluorescence. Excitation wavelength was fixed at 292 nm. The emission spectra were recorded at 25 °C from 290 to 400 nm at a scan rate of 250 nm/min. Maximum emission wavelength (λ_{max}) and fluorescence intensity ratio at 360 nm over 320 nm (rFI 360/320) represent the average of three values obtained from emission spectra that were corrected for blank measurements containing different Ficoll70 concentrations, ranging form 0 to 400 g/L. For calcium titration, aliquots of calcium from 0.1M stock solution in buffer A were progressively added into the cuvette that contained the protein under constant agitation. Thermal-induced denaturation of RC_L at various Ficoll70 concentrations was monitored by the intrinsic fluorescence and scanned from 10 to 95 °C with a temperature increment of 1 °C between each spectrum. Spectra of Ficoll70 at each concentration and at different temperatures were subtracted to protein spectra.

Curve fittings

All fitting procedures were done with Kaleidagraph (Synergy Software, Reading, PA) and have been described previously [1-3].

a- Calcium-induced conformational changes.

The equilibrium dissociation constants were determined from experimental curves of either CD signals or the ratio of fluorescence intensity ($FI_{360/320}$) as a function of calcium concentration. The plots were fitted to a two state model as described elsewhere [1,3].

The effective calcium concentration $\left[Ca^{2+}\right]$ in the samples were determined as:

$$\left[Ca^{2+}\right] = \frac{n_{Ca^{2+}}}{V_C(1-\varphi)},$$

where n_{Ca2+} is the number of mol of calcium added (from a 0.1M stock solution in buffer A) into the cuvette of a sample volume V_C, and φ is the fraction volume occupied by the molecular crowding agent, which is determined using the equation:

$$\varphi = C * (\bar{\nu} + \frac{\delta}{\rho}),$$

where C is the concentration of the molecular crowding agent in g_{ficoll}/L; ν is the partial specific volume in L/g_{ficoll}; δ is the time-average apparent hydration of ficoll in g_{H2O}/g_{ficoll} and ρ is water density in g_{H2O}/L. In this work we computed the excluded volume of Ficoll70 without hydration (δ = 0 g/g), with a hydration of 0.3 and 1 g/g.

b- Thermal-induced unfolding experiments.

The thermal-induced denaturation of RC_L at various Ficoll70 concentrations (from 0 to 400 g/L) were followed by tryptophan intrinsic fluorescence and by synchrotron circular dichroism in the far-UV region. The treatment procedure and the determination of van't Hoff free enthalpy (ΔH_{vH}), temperature of half-melting (T_m), the heat capacity (ΔCp) and free energy of unfolding (ΔG) have been described previously [3] and they were calculated as follows:

The fraction of native protein f_N that populated the native state, N, is given by:

$$f_N = \frac{N}{N+U} = \frac{1}{1+\left(\frac{U}{N}\right)} = \frac{1}{1+K_T},$$

where U is the concentration of RC_L in the thermal-unfolded state and K the equilibrium constant at a given temperature: $K_T = U/N$

The free energy of unfolding ΔG at any temperature is related to the enthalpy ΔH and the entropy ΔS of the unfolding reaction

$\Delta G = \Delta H - T\Delta S$ with $\Delta H = \Delta H_{vH} + \Delta Cp\left(T - T_m\right)$ and $\Delta S = \Delta S_m + \Delta Cp \ln\left(T/T_m\right)$, given

$\Delta G = \Delta H_{vH} + \Delta Cp\left(T - T_m\right) - T\left(\Delta S_m + \Delta Cp \ln\left(T/T_m\right)\right)$, given the Gibbs-Helmholtz equation:

$$\Delta G = \Delta H_{vH} - T\Delta S_m + \Delta Cp\left(T - T_m - T\ln\left(T/T_m\right)\right)$$

where ΔCp is the variation of heat capacity at constant pressure, T_m the temperature of half denaturation (where U=N), ΔH_{vH} and ΔS_m the van't Hoff enthalpy and the entropy changes.

Around T_m, U=N given $K_{Tm} = 1$. The equilibrium constant K being related to the free energy $\Delta G = -RT\ln K$, at the melting temperature: $\Delta G_m = -RT_m \ln K_{Tm} = 0$.

Hence, $\Delta G_m = \Delta H_{vH} - T_m \Delta S_m = 0$ from where ΔS_m can be expressed as follows: $\Delta S_m = \frac{\Delta H_{vH}}{T_m}$ and then the Gibbs-Helmholtz equation is rearranged:

$$\Delta G_m = \Delta H_{vH}\left(1 - \frac{T}{T_m}\right) + \Delta Cp\left(T - T_m - T\ln\left(T/T_m\right)\right) \quad \text{(Eq 1).}$$

From the free energy expression related to the equilibrium constant K, $\Delta G = -RT\ln K$, K is extracted: $K = \exp^{\left(\frac{-\Delta G}{RT}\right)}$. In the vicinity of T_m, $K = \exp^{\left(\frac{-\Delta G_m}{RT}\right)}$, where

$$\frac{-\Delta G_m}{RT} = \frac{\Delta H_{vH}\left(1 - \frac{T}{T_m}\right) + \Delta Cp\left(T - T_m - T\ln\left(T/T_m\right)\right)}{-RT} = \frac{\Delta H_{vH}\left(\frac{1}{T_m} - \frac{1}{T}\right) + \Delta Cp\left(\frac{T_m}{T} - 1 + \ln\left(T/T_m\right)\right)}{R}$$

Finally, the fraction of native RC_L can be expressed as follows, providing ΔH_{vH} ,T_m and ΔCp:

$$f_N = \frac{1}{1+\exp^{\left(\frac{-\Delta G}{RT}\right)}} = \frac{1}{1+\exp^{\left(\frac{\Delta H_{vH}\left(\frac{1}{T_m}-\frac{1}{T}\right)+\Delta Cp\left(\frac{T_m}{T}-1+\ln\left(T/T_m\right)\right)}{R}\right)}}$$

ΔG values shown in Figure 4 are computed from Equation 1.

Similar Tm, ΔH_{vH} and ΔCp where found irrespectively of the protein concentration: at 2.5 μM: Tm= 348 and ΔH_{vH} = 89 Kcal/mol; at 10 μM: Tm= 348 and ΔH_{vH} = 92 Kcal/mol and at 20 μM: Tm= 347 and ΔH_{vH} = 87 Kcal/mol. These data suggest that there is no protein concentration effect on the thermodynamic parameters of holo-RC_L.

c- Determination of the Flory exponent.

Cheung and co-workers [8] proposed a direct relation between the size of the confinement space and the thermal stability of proteins in a crowded environment according to the relation:

$$\Delta T_m = \chi * \varphi^{\frac{\alpha}{3}}$$

where ΔTm is the difference between Tm at a given Ficoll70 concentration minus the Tm in the absence of Ficoll70, χ is a constant including the dimensions of the crowder and of the accessible volume [8,9], φ is the fraction occupied by the crowding agent (calculated as described previously) and α is a factor determined by a linear fitting to the data according to:

$$Ln\Delta T_m = \frac{\alpha}{3} Ln\varphi + Ln\chi$$

The Flory exponent (ν) can then be calculated from the α value [9-12] as follows:

$\nu = \frac{1}{\alpha} + \frac{1}{3}$ for available volume of spherical shape and,

$\nu = \frac{1}{\alpha}$ for available volume of slit shape.

The Flory exponent (ν) is related to the behavior of the macromolecule in a space of defined dimensions (d) according to P. J. Flory [12,13]:

$$\nu = \frac{3}{d+2}$$

Supporting Figures

MHHHHHHTMASARDDVLIGDAGANVLNGLAGNDVLSGGAGDDVLLGDEGS
DLLSGDAGNDDLFGGQGDDTYLFGVGYGHDTIYESGGGHDTIRINAGADQ
LWFARQGNDLEIRILGTDDALTVHDWYRDADHRVEIIHAANQAVDQAGIE
KLVEAMAQYPD

Non RTX-Sequence	**RTX consensus**
	GGXGXDXUX
MHHHHHHT	1530
	MASARDDVLI
	GDAGANVLN
	GLAGNDVLS
	GGAGDDVLL
	GDEGSDLLS
	GDAGNDDLF
	GGQGDDTYLFG
	VGYGHDTIYE
	SGGGHDTIR
	INAGADQLWFARQGNDL
	EIRILGTDDALTVHDWY
	RDADHRVEIIHAANQAV
	DQAGIEKLVEAMAQYPD
	1680

Figure S1. Primary Sequence of RC_L, corresponding to residues 1530-1680 of native adenylate cyclase toxin.

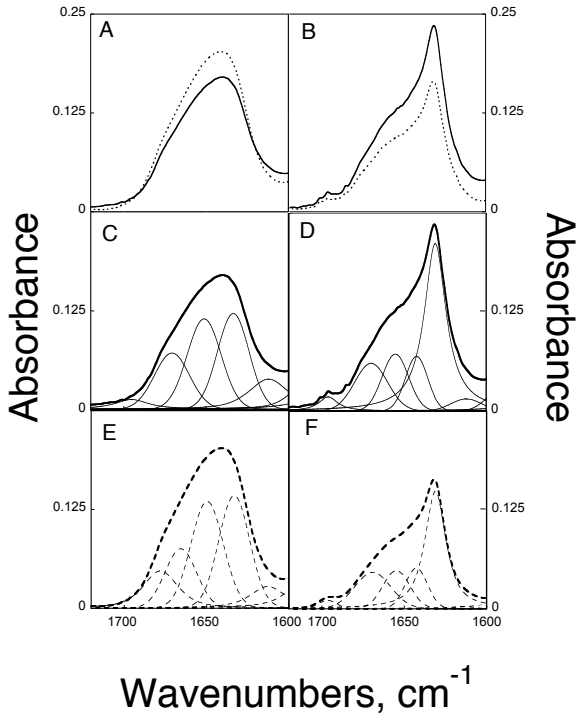

Figure S2. Ficoll70 effect on RC_L followed by FT-IR in the Amide I' region. FTIR absorbance spectra of apo-RC_L (A) and holo-RC_L (B) both in D_2O buffer (continuous line) or in D_2O buffer supplemented with 200 g/L of Ficoll70 (dashed line). C and E, Deconvolution-curve fitting of the amide I' band of apo-RC_L in the absence or in the presence of 200 g/L of Ficoll70, respectively. D and F, Deconvolution-curve fitting of the amide I' band of holo-RC_L in the absence or in the presence of 200 g/L of Ficoll70 respectively. Secondary structure determination was performed by the deconvolution-curve fitting of the nondeconvolved spectra in the amide I' region of RC_L. Experimental conditions: D_2O buffer A supplemented with 5 mM calcium for holo experiments, 25 °C. Polypeptide concentration ranged from 1 to 5 mg/mL.

In the absence as in the presence of Ficoll70 (Supporting Fig S2A), the amide I' band of apo-RC_L presented a maximum absorption wavenumber (ν_{max}) at 1645 cm^{-1}, typical of random coils (Supporting Table S1, [6,7]), with a shoulder between 1660 and 1680 cm^{-1}, suggesting the presence of some turns. The FTIR spectra were deconvoluted by curve fitting procedures (see material and methods and Supporting Fig. S2C and S2E) to quantitatively compare the secondary structure content of apo-RC_L in the absence and in the presence of 200g/L of Ficoll70 (Supporting Table S1). In both cases, the apo-state was mainly composed of disordered regions with few turns and β-sheets, thus confirming that Ficoll70 was not able to induce secondary structure folding of RC_L, in agreement with CD data.
The FTIR spectra of the holo-state (Supporting Fig. 2B) exhibit a major band located at 1627 cm^{-1} characteristic of parallel β-sheets. Spectra deconvolution (Figures S2D and S2F) showed that calcium-binding to RC_L was characterized by a strong increase of β- sheet content at the expense of the random

coil content. Similarly to what we observed in the apo-state, the presence of 200 g/L of Ficoll70 did not significantly affect the FTIR spectrum of the holo-state of RC_L.

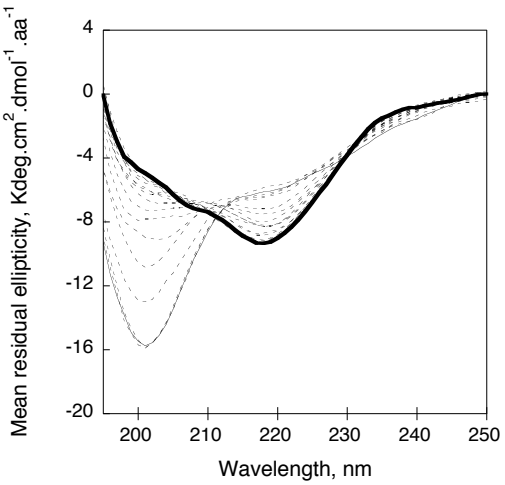

Figure S3. Far-UV SR-CD spectra of holo-RC_L as a function of temperature in the absence of Ficoll70. Holo-RC_L at 25 °C is bold and at 95°C is showed as a continuous line.

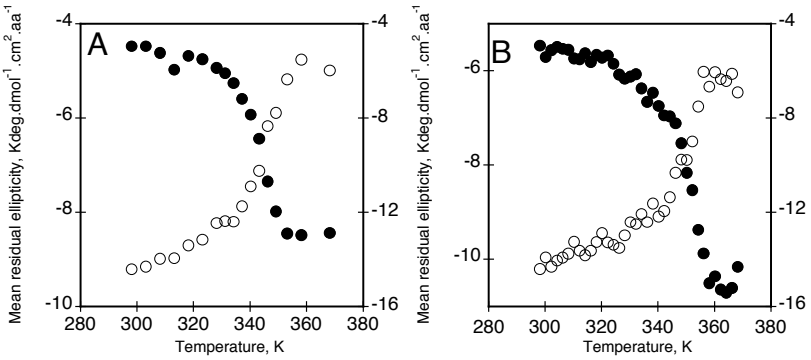

Figure S4. Thermal unfolding of holo-RC_L followed by far-UV SRCD at 201 nm (●) and at 218 nm (○) in the absence (panel A) or in the presence (panel B) of 200 g/L of Ficoll70. Experimental conditions: buffer A + 5 mM calcium. Polypeptide concentration was 3.5 mg/mL .

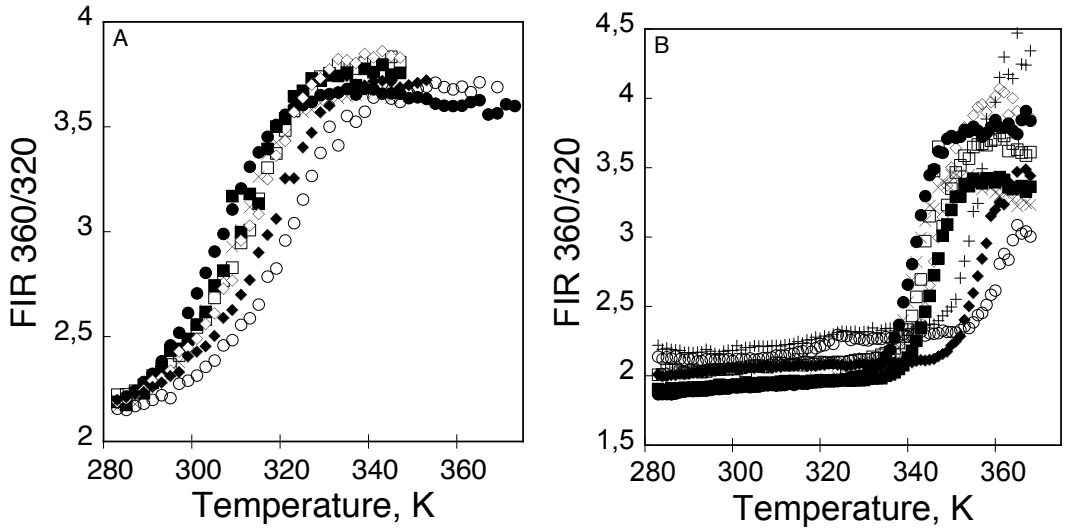

Figure S5. Effect of Ficoll70 on the thermal stability of RC_L followed by tryptophan intrinsic fluorescence. Thermal denaturation of apo-RC_L (A) and holo-RC_L (B) followed by $FIR_{360/320}$ in buffer containing 0 g/L (●); 50 g/L (X); 100 g/L (■); 150 g/L (□); 200 g/L (◇); 250 g/L (+); 300 g/L (◆); and 400 g/L (○) of Ficoll70. Experimental conditions: buffer A +/- 2 mM calcium. Polypeptide concentration was 10 μM.

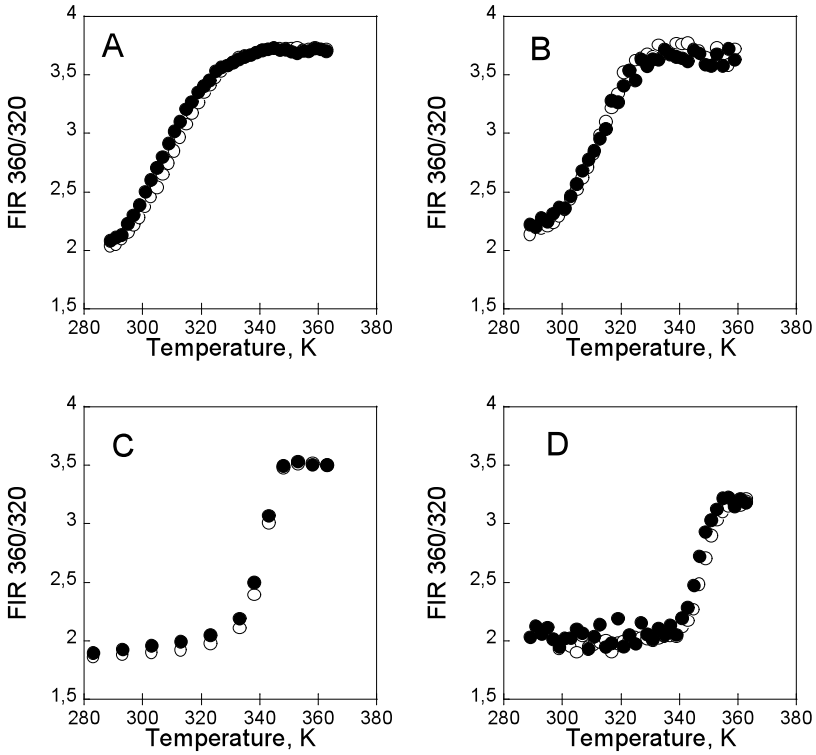

Figure S6. Thermal unfolding (○) and refolding (●) of RCL in the absence (A and C) or in the presence (B and D) of 200 g/L of Ficoll70 followed by $FIR_{360/320}$. Experimental conditions: buffer A ± 200 g/L Ficoll70 ± 2 mM calcium. Polypeptide concentration ranges from 2 to 10 μM.

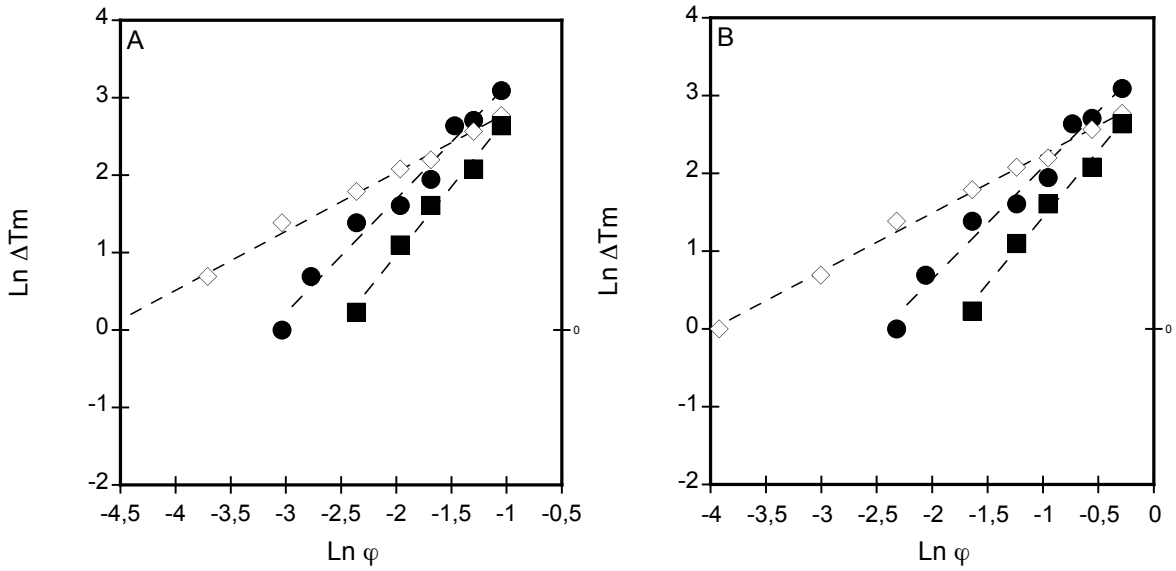

Figure S7. Ficoll70 effect on the melting temperature ΔTm as a function of excluded volume φ_C considering dry spherical molecules of Ficoll70 (panel A) and hydrated (1 g/g) Ficoll70 (panel B). Data come from apo-RC_L (◇) and holo- RC_L (●) thermal denaturation followed by tryptophan intrinsic fluorescence and holo- RC_L (■) thermal denaturation followed by SR-CD in the far-UV region.

Supporting Table S1. Assignment of amide I' bands to the secondary structure content of RTX polypeptide in the absence and presence of ficoll.

	Buffer		Ficoll 200 g/L	
Assignment	[1]Apo-RTX, %	[2]Holo-RTX, %	[1]Apo-RTX, %	[2]Holo-RTX, %
Beta-sheets (1)	22	38	20	34
Alpha	-	13	-	13
Random	40	17	41	19
Turn	29	25	35	30
Beta-sheets (2)	9	7	4	4

[1] In the absence of calcium

[2] In the presence of 5 mM $CaCl_2$

Supporting Table S2. Effect of Ficoll hydration on the equilibrium calcium dissociation constant of RC_L.

	Ficoll 0 g/L	**Ficoll 100 g/L**	**Ficoll 200 g/L**	**Ficoll 300 g/L**	**Ficoll 400 g/L**
K_D[1] δ = 0 g/g	530	380	340	280	225
K_D[2] δ = 0.3 g/g	530	390	365	320	275
n_H[3]	3.5	4.0	3.5	3.9	3.4

[1,2] K_D^{Ca2+} : Equilibrium dissociation constants (μM) calculated considering the partial specific volume ($\bar{v}$) and hydration (δ) of ficoll as described in Material and Methods. All values are results of at least 3 independent determinations with a Standard deviation lower than 0.02 mM.

[3] nH : Hill number

Supporting Table S3. Thermodynamic parameters (Tm, in Kelvin; $\Delta H_{vH,}$ in kcal/mol; ΔCp in kcal/mol/K and ΔG in kcal/mol) as a function of Ficoll70 concentration.

	Holo RC_L										**Apo RC_L**				
	Circular Dichroism					**Fluorescence Spectroscopy**					**Fluorescence Spectroscopy**				
Ficoll g/L	**ΔH**	**Tm**	**ΔCp**	**ΔG 25°C**	**ΔG 37°C**	**ΔH**	**Tm**	**ΔCp**	**ΔG 25°C**	**ΔG 37°C**	**ΔH**	**Tm**	**ΔCp**	**ΔG 25°C**	**ΔG 37°C**
0	33	344	2.1	4.3	3.2	39	341	1.8	4.9	3.6	10	303	0.7	0.16	-0.23
10											11	304	0.8	0.20	-0.21
25						47	341	2.3	5.9	4.3	13	305	0.9	0.29	-0.21
50						45	342	2.1	5.7	4.2	12	307	0.74	0.36	-0.12
65						50	343	2.4	6.5	4.8					
100	37	343	2.3	4.8	3.6	44	345	1.9	6	4.4	11	309	0.7	0.33	-0.11
150						44	346	1.8	6.1	4.5	12	311	0.66	0.50	0.04
200	39	350	2.2	5.8	4.4	44	348	1.8	6.3	4.8	12	312	0.64	0.53	0.08
250						44	355	1.8	7.0	5.6					
300						45	356	1.7	7.3	5.8	13	316	0.67	0.73	0.24
400	39	357	2.4	6.4	5.1	47	363	2	8.4	6.9	12	319	0.56	0.81	0.35

Standard deviation of Tm values is ± 1K; S.D. on ΔH is less than 5 kcal/mol.

Table S4. Parameters obtained from fitting the data in Figures 5 and S7 as described in material and methods, using both spherical and slit available volume models.

	Holo RC_L						**Apo RC_L**		
	Circular Dichroism			**Fluorescence Spectroscopy**					
δ, g/g	α	ν slit	ν sphere	α	ν slit	ν sphere	α	ν slit	ν sphere
0	5.28	0.19	0.53	4.41	0.23	0.56	2.28	0.44	0.77
0.3	5.21	0.19	0.52	4.36	0.23	0.56	2.26	0.44	0.77

(1) Sotomayor Perez, A. C.; Karst, J. C.; Davi, M.; Guijarro, J. I.; Ladant, D.; Chenal, A. *J Mol Biol* **2010**, *397*, 534.
(2) Sotomayor-Perez, A. C.; Ladant, D.; Chenal, A. *J Biol Chem* **2011**, *286*, 16997.
(3) Chenal, A.; Karst, J. C.; Sotomayor Perez, A. C.; Wozniak, A. K.; Baron, B.; England, P.; Ladant, D. *Biophys J* **2010**, *99*, 3744.
(4) Barth, A. *Biochim Biophys Acta* **2007**, *1767*, 1073.
(5) Barth, A.; Zscherp, C. *Q Rev Biophys* **2002**, *35*, 369.
(6) Goormaghtigh, E.; Cabiaux, V.; Ruysschaert, J. M. *Subcell Biochem* **1994**, *23*, 405.
(7) Goormaghtigh, E.; Cabiaux, V.; Ruysschaert, J. M. *Subcell Biochem* **1994**, *23*, 329.
(8) Cheung, M. S.; Klimov, D.; Thirumalai, D. *Proc Natl Acad Sci U S A* **2005**, *102*, 4753.
(9) Waegele, M. M.; Gai, F. *J Chem Phys* **2011**, *134*, 095104.
(10) de Gennes, P. G. *Scaling Concepts in Polymer Physics*; Cornell university Press: Ithaca, NY, 1979.
(11) Flory, P. J.; Krigbaum, W. R. *Journal of Chemical Physics* **1950**, *18*, 1086.
(12) Sakaue, T.; Raphaël, E. *Macromolecules* **2006**, *39*, 2621.
(13) Flory, P. J.; Cornell University Press, I., N. Y., Ed. 1953.